Official journal of the American Society of Gene & Cell Therapy

MTOpen

original article

Human Mesenchymal Stem Cells Genetically Engineered to Overexpress Brain-derived Neurotrophic Factor Improve Outcomes in Huntington's Disease Mouse Models

Kari Pollock[1], Heather Dahlenburg[1], Haley Nelson[1], Kyle D Fink[1], Whitney Cary[1], Kyle Hendrix[1], Geralyn Annett[1], Audrey Torrest[1], Peter Deng[1], Joshua Gutierrez[1], Catherine Nacey[1], Karen Pepper[1], Stefanos Kalomoiris[1], Johnathon D Anderson[1], Jeannine McGee[1], William Gruenloh[1], Brian Fury[1], Gerhard Bauer[1], Alexandria Duffy[2], Theresa Tempkin[2], Vicki Wheelock[2] and Jan A Nolta[1]

[1]Stem Cell Program and Institute for Regenerative Cures, University of California Davis Health System, Sacramento, California, USA; [2]Department of Neurology, University of California Davis Health System, Sacramento, California, USA

Huntington's disease (HD) is a fatal degenerative autosomal dominant neuropsychiatric disease that causes neuronal death and is characterized by progressive striatal and then widespread brain atrophy. Brain-derived neurotrophic factor (BDNF) is a lead candidate for the treatment of HD, as it has been shown to prevent cell death and to stimulate the growth and migration of new neurons in the brain in transgenic mouse models. BDNF levels are reduced in HD postmortem human brain. Previous studies have shown efficacy of mesenchymal stem/stromal cells (MSC)/BDNF using murine MSCs, and the present study used human MSCs to advance the therapeutic potential of the MSC/BDNF platform for clinical application. Double-blinded studies were performed to examine the effects of intrastriatally transplanted human MSC/BDNF on disease progression in two strains of immune-suppressed HD transgenic mice: YAC128 and R6/2. MSC/BDNF treatment decreased striatal atrophy in YAC128 mice. MSC/BDNF treatment also significantly reduced anxiety as measured in the open-field assay. Both MSC and MSC/BDNF treatments induced a significant increase in neurogenesis-like activity in R6/2 mice. MSC/BDNF treatment also increased the mean lifespan of the R6/2 mice. Our genetically modified MSC/BDNF cells set a precedent for stem cell-based neurotherapeutics and could potentially be modified for other neurodegenerative disorders such as amyotrophic lateral sclerosis, Alzheimer's disease, and some forms of Parkinson's disease. These cells provide a platform delivery system for future studies involving corrective gene-editing strategies.

Received 9 August 2015; accepted 5 December 2015; advance online publication 15 March 2016. doi:10.1038/mt.2016.12

INTRODUCTION

Huntington's disease (HD) is a fatal, degenerative autosomal dominant neuropsychiatric disease that afflicts nearly one in 10,000 people in the United States. HD is caused by an expanded CAG trinucleotide repeat region located in exon 1 of the huntingtin gene. The HD mutation causes neuronal death and is characterized initially by striatal atrophy with later generalized brain atrophy.[1] Clinical symptoms include progressive cognitive decline, psychiatric symptoms, and chorea. Currently available medications are strictly palliative and target only some symptoms of the disease, such as chorea and psychiatric features.[2–4] There are no available treatments to attenuate the underlying neuronal cell death and subsequent striatal atrophy seen in HD.

Previous studies have shown brain-derived neurotrophic factor (BDNF) to be a putative candidate for the treatment of HD. BDNF is known to mediate both the survival and function of striatal neurons.[5] Both cortical and striatal BDNF levels are reduced in postmortem HD brain[6,7] due to inhibition of BDNF expression levels at the transcriptional level by the mutant huntingtin protein. This reduction in BDNF in the striatum correlates with symptom onset and heightened severity of the disease in transgenic HD mice.[5] BDNF knockout mice recapitulate the striatal atrophy phenotype of HD patients and indicate that reduced neurotrophic support in the striatum is a major factor contributing to neurodegeneration in HD.[8] BDNF expression levels are lowered in transgenic mouse models of HD and the restoration of BDNF expression levels has been shown to have prosurvival effects on neurons and ameliorate HD symptoms.[5,9–35] Therefore, BDNF is considered a prime candidate to treat the underlying neuronal loss seen in HD (reviewed in refs. [36,37]).

Effective delivery of BDNF for neurological disorders remains a major challenge due to its very short half-life, which severely limits the effectiveness of the recombinant protein. Several studies have examined various exogenous delivery methods that may be utilized to translate BDNF based therapeutics to the clinic.

Correspondence: Jan A Nolta, Stem Cell Program and Institute for Regenerative Cures, University of California, Davis, 2921 Stockton Blvd., Room 1300, Sacramento, California 95817, USA. E-mail: Janolta@ucdavis.edu

Benraiss *et al.*[20] used adeno-associated virus (AAV) vectors to express BDNF in striatal neurons and demonstrated that AAV delivery of BDNF-induced neurogenesis and promoted a longer lifespan in a murine model of HD. Interestingly, this benefit was potentiated by a factor secreted by mesenchymal stem/stromal cells (MSCs), noggin.[38–41] However, efforts to translate AAV vector therapeutics in the clinic have been hampered by their immunogenic properties.

The Dunbar laboratory has shown murine MSCs engineered to overexpress BDNF had significant ameliorative effects on disease progression in a transgenic mouse model of HD.[27] These studies demonstrated that murine MSC/BDNF implanted into the striata significantly increased improved motor performance and reduced HD associated movement disorders.[27] The present study used human MSCs to advance the therapeutic potential of the MSC/BDNF platform for potential clinical application.

MSCs were chosen as the delivery platform for BDNF since they are known to secrete a variety of neurotrophic and other factors that reduce inflammation, reduce programmed cell death, enhance connections between neurons, and reduce cell toxicity.[42] MSCs have been shown to be readily engineered using viral vectors to robustly deliver growth factors.[43,44] Using gene-modified MSCs as a delivery strategy addresses certain safety concerns involved with the direct use of viral vectors, as MSCs do not permanently engraft into host tissues. In addition, MSCs do not require immunosuppression following allogeneic transplantation, and have a strong, demonstrable safety profile in clinical trials.[45–53]

MSC/BDNF combines the beneficial effects of BNDF administration to the striata along with the benefits of MSC secreted factor supplementation (*e.g.*, noggin). Unlike direct BDNF delivery via viral vector injection or recombinant protein administration into the brain, MSCs migrate into areas of tissue damage and have been shown to have numerous tissue healing effects (reviewed in ref. [42]). Studies have shown MSCs do not permanently engraft into host tissues; however, the duration and strategic localization of BDNF production should be adequate to produce a beneficial effect in the HD striata by promoting neurogenesis. We hypothesize that the neurorestorative effects of BDNF will outlast the survival of MSCs. This is supported by animal data from our laboratory and others.[20,27,54–60]

The YAC128 mouse model was used in the behavioral and striatal volume studies. This strain provides expression of a full length human huntingtin gene with 128 CAG repeats. The YAC128 strain is an excellent model for HD which recapitulates the slow decline in motor and behavioral function and the progressive striatal loss and neuropathology that are seen in human HD. Motor, striatal and behavioral deficits are not seen until 7–12 months in this strain. We used this strain with immune suppression to measure the attenuation of striatal decline by a cell therapy candidate, MSC/BDNF. We also used it to measure a decrease in overall anxiety caused by our cell therapy product, as measured in the open-field assay.

The R6/2 strains have rapid onset and progression. We performed neurogenesis assays in the R6/2 (CAG 120) mouse model of HD due to their early disease progression and very rapid decline, which is more like the rapidly progressing juvenile HD (JHD), than adult HD. The R6/2 strain only lives for 13–17 weeks in our colony, making repeated measures after immune suppression and surgery difficult. However, they are a useful HD strain for measuring the effects of MSC/BDNF and other agents on neurogenesis.

In order for therapies to be effectively translated into the clinic, safety and efficacy must first be demonstrated in preclinical animal studies. However, efficacy testing of human stem cell therapeutics in transgenic mouse models is challenging as human cells can be rejected from immune competent mice via a xenogeneic immune response. Currently, no immune-deficient mouse models of HD exist; therefore, we used an immunosuppressive regimen (FK506 and rapamycin) which permitted retention of human MSC/BDNF cells up to 28 days postimplantation, which was similar to the results observed in the severely immunodeficient NOD/SCID/Gamma chain -/- (NSG) strain. Development of this immune suppression regimen permitted efficacy testing of the MSC/BDNF in two immunocompetent transgenic animal models of HD, YAC128, and R6/2.

Our data demonstrate that intrastriatal delivery of human MSC/BDNF significantly reduced anxiety-like behaviors and significantly increased neurogenesis in immune suppressed HD mouse models, with a trend toward increased survival. A significant decrease in striatal volume was striatal volume was observed between vehicle-treated HD mice and wild type mice, but was not observed in the HD mice that received MSC/BDNF. This recovery may be due to the stimulation and maturation of endogenous neurogenesis promoted by BDNF, and enhanced by the secretion of various complementary therapeutic factors by MSCs.

RESULTS

MSC/BDNF: vector integration and characterization

Human MSCs were obtained from the bone marrow of qualified allogeneic donors and were engineered to secrete elevated levels of BDNF via lentiviral transduction. The use of lentiviral transduction ensures consistent, sustained expression of BDNF for the duration of the survival of these cells within the striata. In addition, clinical products must be consistent from batch to batch to ensure consistency of any therapeutic benefit, which can be ensured by lentiviral transduction using a standardized titer at a fixed, experimentally determined multiplicity of infection (MOI).

A schematic of the lentiviral vector used in the current studies, pCCLc-MNDU3-BDNF-WPRE is shown in **Figure 1a**. pCCLc was used as the backbone for this third generation lentiviral vector, as originally described by Dull *et al.*[61] The MNDU3 promoter was generated in the laboratory of Dr. Donald Kohn and consists of the U3 region of the MND oncoretroviral vector.[62] The MNDU3 promoter is a strong promoter and particularly useful for constitutive expression of proteins. It has already been used as a retroviral vector backbone in a stem cell gene therapy clinical trial for adenosine deaminase (ADA) deficiency without adverse events, over a 10-year follow-up period in hematopoietic stem cells.[63] Woodchuck postregulatory element (WPRE), the woodchuck hepatitis virus post-transcriptional regulatory element, increases mRNA levels post-transcriptionally, but is not likely to activate any oncogene, as it is not a promoter.

This BDNF expression vector was used to transduce human bone marrow derived MSCs at increasing MOI. Subsequently, integration rates were assessed. To determine whether there were any deletions or rearrangements in vector-transduced cells, genomic polymerase

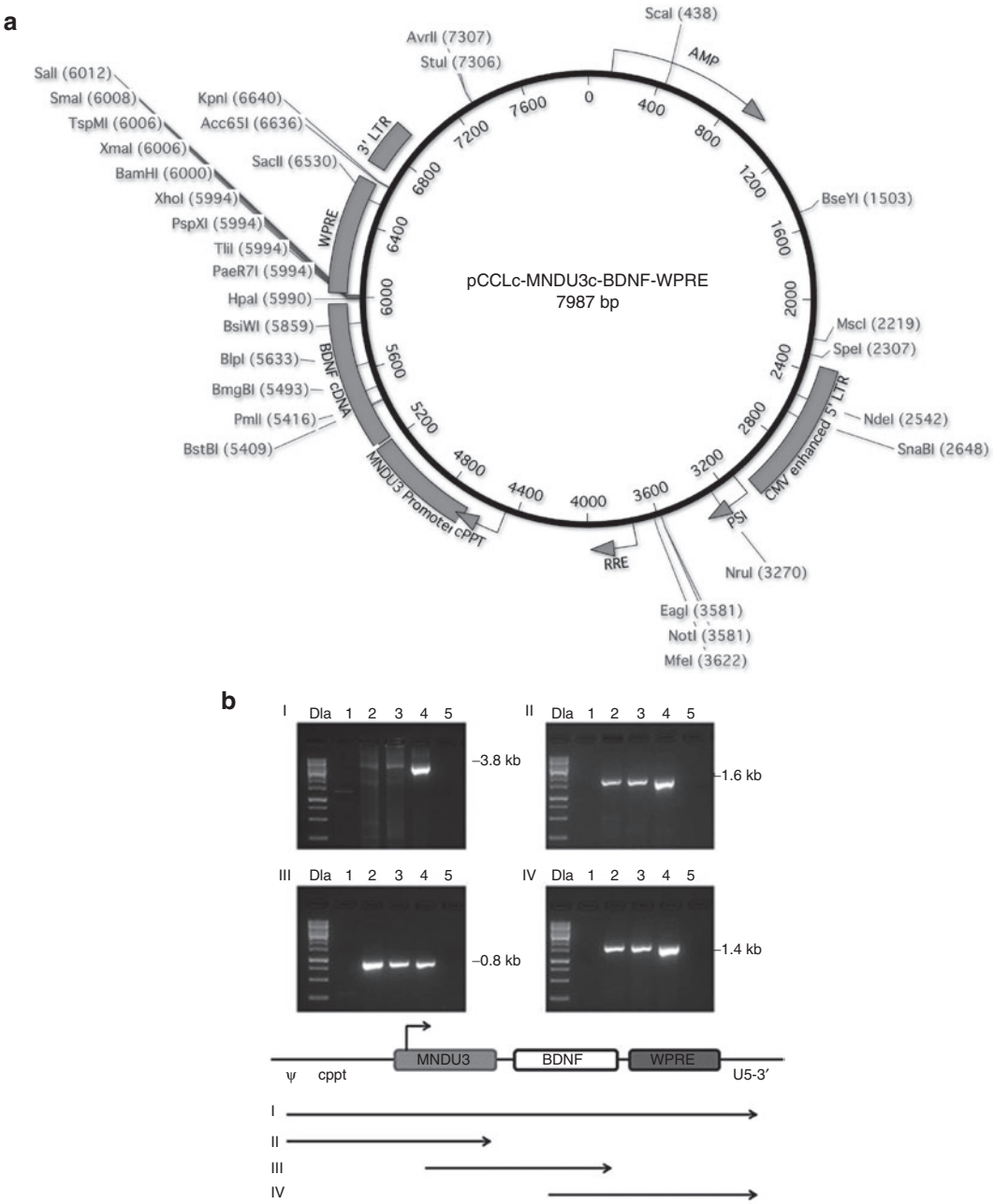

Figure 1 Vector map and stability. (**a**) Vector map diagram for pCCLc-MNDU3-BDNF-WPRE. A third-generation lentiviral vector, based on the pCCLc-x backbone was used to generate a BDNF gene construct. The transgene is driven by the MNDU3 promoter, a constitutive RNA polymerase II promoter. BDNF is the gene encoding brain-derived neurotrophic factor, cloned in our lab from adult human bone marrow-derived MSCs. WPRE is the woodchuck hepatitis post-transcriptional regulatory element, which acts in cis to enhance gene expression. (**b**) Stability of the clinical vector in transduced cells. To determine whether there were any deletions or rearrangements in vector-transduced cells, genomic PCR was performed. MSCs were transduced with the BDNF vector at MOI 10 or MOI 20. Total genomic DNA was extracted and analyzed by PCR with primers specific for the respective vector segments. (**I**) ψ (forward) and U5-3′ (reverse), (**II**) ψ (forward) and MNDU3 (reverse), (**III**) MNDU3 (forward) and BDNF (reverse), and (**IV**) BDNF (forward) and U5-3′ (reverse). Resulting DNA was run on a gel in the following lanes: 1 kb DNA ladder (DLa), nontransduced MSCs (negative control, lane 1), BDNF MOI 10 MSCs (lane 2), BDNF MOI 20 MSCs (lane 3), BDNF vector plasmid (positive control, lane 4), no template control (lane 5). Bands were of the expected size, as shown in the schematic of the PCR products below the panels. Ψ, psi packaging sequence; BDNF, brain-derived neurotrophic factor; WPRE, woodchuck hepatitis virus post-transcriptional regulatory element.

chain reaction (PCR) was performed. The stability of our integrated BDNF lentiviral vector was evaluated by PCR with genomic DNA from transduced cells. The BDNF transgene was continuously present after integration and structurally stable (**Figure 1b**). Bands were of the expected size, as shown in the schema.

BDNF production

MSC/BDNF cells were thawed and incubated in 20% O_2 for 24 hours, followed by incubation in 1% O_2 for 48 hours. No differences in morphology or rate of senescence were detected between gene-modified cells (MSC/BDNF) and unmodified MSCs (**Figure 2a**).

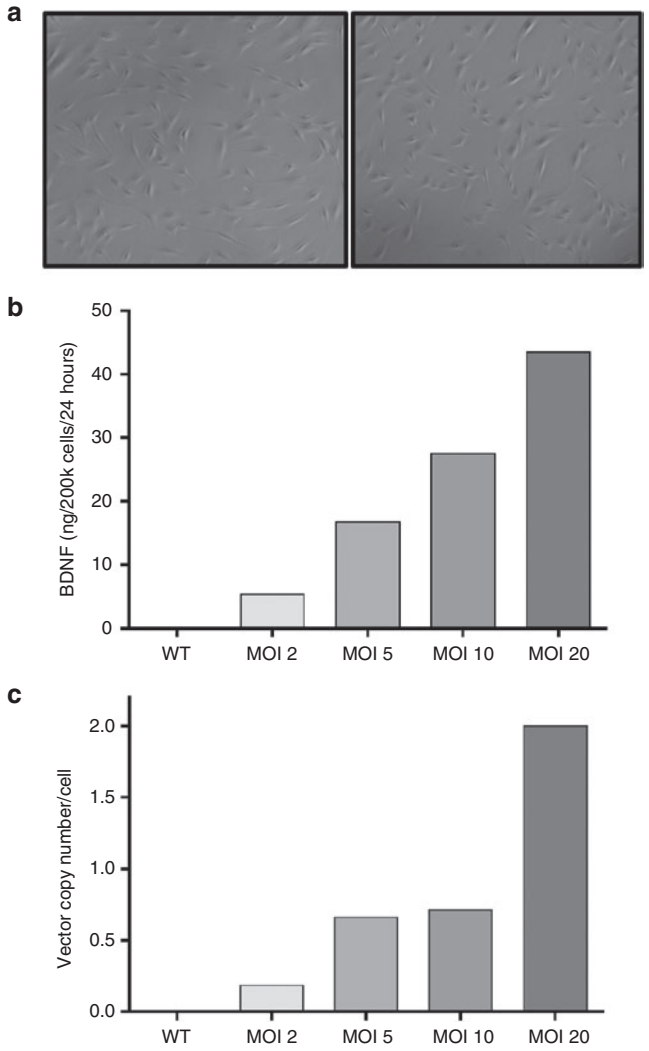

Figure 2 Cell characterization. (**a**) Cells transduced by the BDNF vector (right), display the size and phenotypic appearance of healthy nontransduced MSCs from the same donor (left). (**b**) *In vitro* characterization showed that human MSCs transduced with the pivotal BDNF lentiviral vector at multiplicities of infection (MOI) 2, 5, 10, and 20 displayed a positive correlation between BDNF production and MOI. Supernatant was collected for determination of secreted BDNF by ELISA after conditioning serum free media for 24 hours. (**c**) Vector copy number at increasing MOI. Human MSCs were transduced with pCCLc-MNDU3-BDNF-WPRE, cryopreserved, then subsequently thawed and expanded for 3 days. DNA was isolated and used for qPCR analysis. Quantification was based on standard curves of plasmid DNA. Vector copy number/cell was determined as WPRE/2GAPDH.

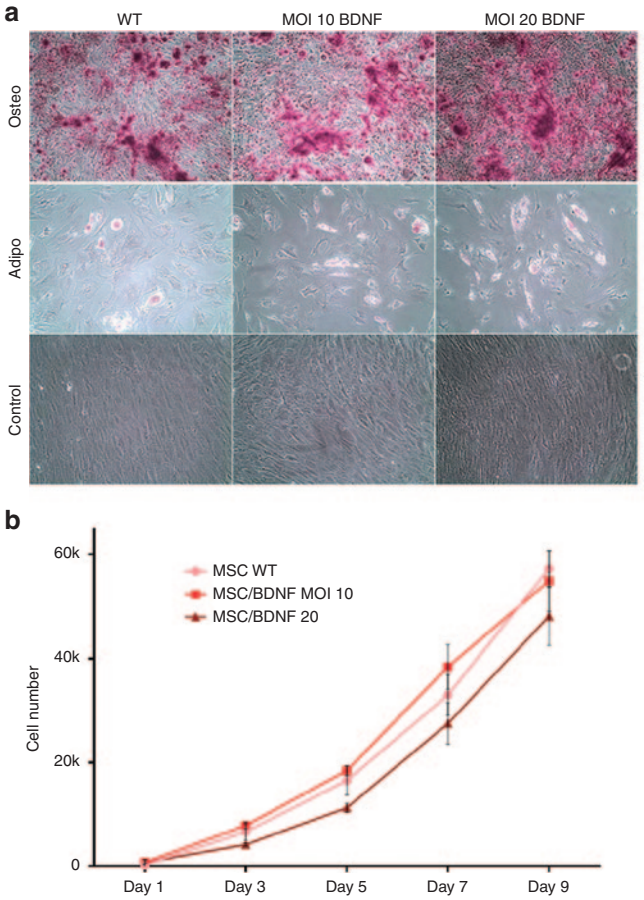

Figure 3 Cell differentiation and proliferation. (**a**) Differentiation potential of MSC is not affected after genetic modification by the BDNF vector. Osteogenesis was assessed by Alizarin Red Staining of precipitated calcium after 16 days in culture in osteogenic media. Representative images (10×) are shown. Adipogenesis was assessed after 16 days in adipogenic media by formation of adipocytes using Oil Red O to stain triglycerides. Representative images (10×) are shown. (**b**) Proliferation rates were not significantly altered in MSCs post-transduction. Passage 6 MSCs were plated at approximately 1,000 cells/cm^2 in 24-well plates and cultured as described. After 1, 3, 5, 7, and 9 days in culture, plates were analyzed using CellTiter96 nonradioactive cell proliferation assay (Promega).

Media was changed to serum-free media after 24 hours in 1% O_2 and the resulting conditioned media was collected for ELISA after an additional 24 hours (**Figure 2b**). As expected, we observed increased BDNF production by MSC/BDNF as we increased the MOI. The MSC/BDNF MOI 10 cell bank generated for use in our efficacy studies produced 10.9 ng of BDNF per 2×10^5 cells in 24 hours (MOI 20 produced 18.1 ng of BDNF per 2×10^5 cells in 24 hours).

Vector copy number and post-transduction MSC/BDNF characterization

Human MSCs were transduced with pCCLc-MNDU3-BDNF-WPRE, cryopreserved, thawed and expanded for 3 days. DNA was isolated and used for qPCR analysis. Quantification was based on standard curves of plasmid DNA. Vector copy number/cell was determined as WPRE/2GAPDH, since WPRE is found only in the vector and each cell has two copies of the GAPDH gene. The MOIs of 10 and 20 produced MSC/BDNF with optimal BDNF levels, as shown in **Figure 2b**, and resulted in 0.5–2 integrated copies of vector DNA per cell, which falls within recommendations provided by the Food and Drug Administration (**Figure 2c**).

To confirm that the differentiation potential of MSC/BDNF cells was not affected by transduction, we performed osteogenic and adipogenic differentiation assays of both transduced and nontransduced MSCs. As shown in **Figure 3a**, we observed similar levels of osteogenesis and adipogenesis across both transduced and nontransduced MSCs. In addition, there were no observed differences in cell proliferation between these cell populations (**Figure 3b**). In summary, no alterations in phenotype, morphology, proliferation rate, or differentiation capacity were observed

in MSCs transduced by the lentiviral vector carrying the BDNF transgene, as compared to nontransduced MSCs.

In vivo retention studies

We tested the safety and efficacy of the human MSC/BDNF cells in two murine models of HD: YAC128 and R6/2. Since xenografts induce a potent immune response, efficacy studies should generally be performed in an immune deficient model; however, an immune deficient mouse model of HD does not currently exist. To address this we used an immune suppressive drug regimen (FK506 and Rapamycin) with both immunocompetent murine models of HD. Retention of intracranially transplanted MSCs was assayed with and without immune suppression (FK506/Rapa by Alzet osmotic pump) and compared to retention in the immune-deficient mouse strain, NSG.

The NSG mouse strain is a highly immune-deficient mouse model and an excellent tool for the testing of human cell-based therapies. The NSG mouse is deficient in mature T and B cells, natural killer cells, serum immunoglobulin, a hemolytic complement system, and has shown the ability to stably engraft many types of human cells. For these reasons, we used NSG mice as positive controls in our retention assays.

Human MSCs were transduced by a lentiviral vector carrying the luciferase gene (pCCLc-MNDU3-Luc-PGK-EGFP-WPRE), which allows cells to be visualized in the brains of living mice over time using IVIS imaging. Mice received unilateral (left) intrastriatal injections of 2.5×10^5 cells and were subsequently imaged on days 2, 4, 7, 14, 21, and 28 postimplantation. As shown in **Figure 4**, human MSCs survived only 1 week in the brains of nonimmune suppressed mice. This rapid clearance occurred in spite of the fact that MSCs can shelter themselves from the immune system, to some extent. The immune privilege capacities of MSCs did not extend across species in our study.

In the immune-suppressed mice, MSCs could be detected in some mice for up to 28 days postimplantation, which was similar to the results observed in the immune-deficient NSG mouse control strain.

MSC/BDNF efficacy: behavioral

To evaluate the behavioral therapeutic effects of MSC/BDNF treatment in YAC128 HD mice, we performed the open-field assay. Among other behavioral outcomes measured, the open-field assay measures anxiety-related behavior, which is a major debilitating problem in HD. All YAC128 mice in the study were immune suppressed using FK506/Rapamycin delivered by an Alzet osmotic pump, as described in **Figure 4**. Mice were then implanted with vehicle, MSC, or MSC/BDNF at 8 ½ months of age, as most behavioral deficits are not apparent in the YAC128 strain until 7–12 months of age. Behavioral testing was conducted weekly following cell implantation for 6 weeks, or until 10 months of age. Mice were then euthanized and brains were collected for histological analysis.

No motor deficits were observed in YAC128 mice during open-field testing, as measured by the total distance traveled,

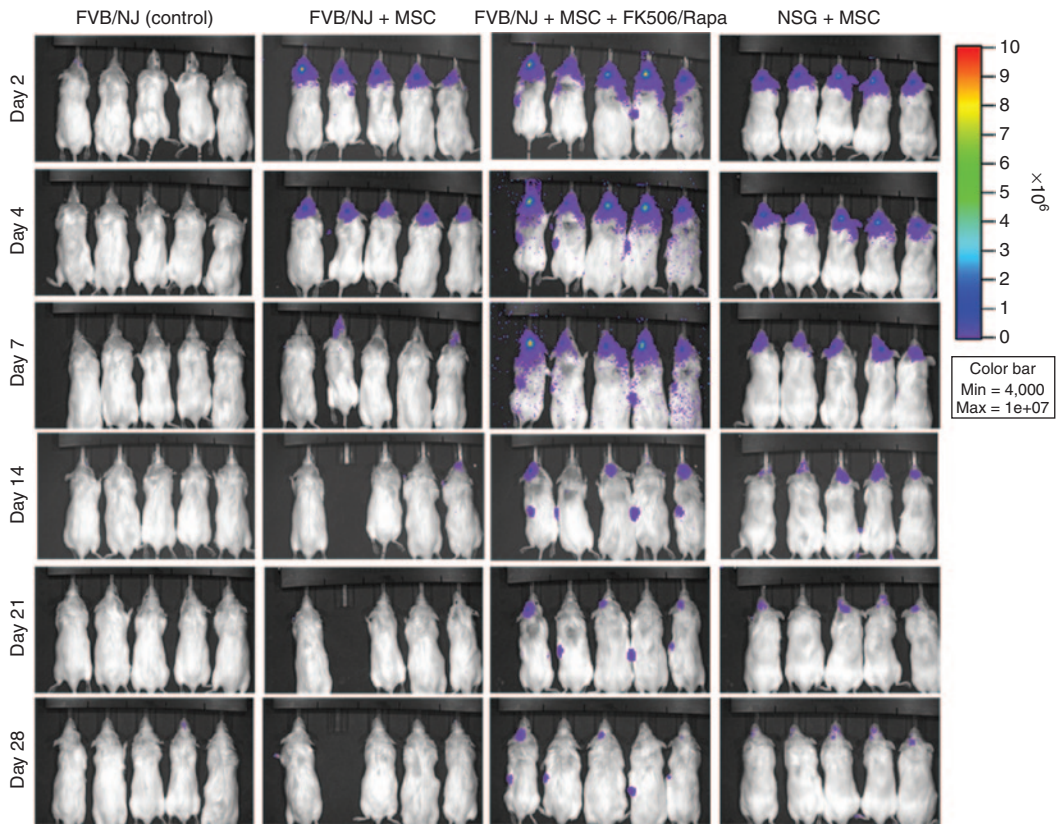

Figure 4 *In vivo* imaging demonstrates that immune suppression (of FVB/NJ mice) was able to increase cell retention to levels similar to that observed in immune-deficient NSG mice for at least 28 days. Human MSCs were transduced by a lentiviral vector carrying the luciferase gene (pCCLc-MNDU3-Luc-PGK-EGFP-WPRE), which allows cells to be visualized (bioluminescence) in the brains of living mice over time.

total movement time, number of exploratory vertical episodes, or number of stereotypic behaviors, (**Figure 5a** and data not shown). These data show that none of the tested groups displayed motor deficits during the time tested. Repeated measures analysis of variance revealed no significant between-group differences for total distance traveled ($F(3,51) = 0.438$, $P = 0.727$), total movement time ($F(3,51) = 2.537$, $P = 0.067$), number of exploratory vertical episodes ($F(3,51) = 0.836$, $P = 0.480$), or number of stereotypic behaviors ($F(3,50) = 1.596$, $P = 0.202$). This suggests that all mice exhibited similar spontaneous exploration of the box and that any differences observed in other behaviors was not due to motor impairment.

Anxiety is a hallmark symptom of HD in humans.[64–66] In murine models, anxious mice spend less time in the center quadrant of an open field as anxiety increases. WT mice avidly explore the center of the open field, whereas transgenic HD mice move along the edges of box and only rarely leave this zone. This behavior is analogous to fear or anxiety in humans. Sham-treated HD mice spent much less time in the center quadrant of the open field as compared to wild type controls, indicating the HD mice were displaying higher levels of anxiety as expected. This display of anxiety is attenuated in HD mice that were treated with MSC/BDNF (**Figure 5b**). Repeated measures analysis of variance revealed a significant between-group difference ($F(3,50) = 4.305$, $P = 0.009$). LSD *post hoc* analysis revealed a significant overall between group difference between WT mice and Tg + Normosol ($P = 0.007$), and Tg + MSC ($P = 0.002$). LSD *post hoc* analysis also revealed an overall between group trend between Tg + Normosol and tg + BDNF hMSC ($P = 0.169$). *Post hoc* one-way analysis of variance (ANOVA) was used to analyze differences between groups at various time points. Significant differences were observed between: WT and Tg + Normosol at baseline at weeks 2, 3, 5, 6, and 7; WT and Tg + MSC BDNF MOI 10 at baseline, and at week 3; WT and Tg + MSC at baseline at weeks 1, 2, 3, 5, and 6; Tg + Normosol and Tg + MSC BDNF MOI 10 on weeks 2 and 7; between Tg + MSC and Tg + MSC BDNF MOI 10 on weeks 2 and 5. This is a significant key behavioral improvement between the YAC128 MSC/BDNF-treated group and the YAC128 sham treatment control. These data demonstrate a significant behavioral amelioration in HD mice receiving MSC/BDNF (**Figure 5**). With distance traveled not significantly different across treatment groups, the significant increase in time in center for transgenic mouse treated with MSC/BDNF indicates a decrease in anxiety rather than purely an increase in locomotor activity.

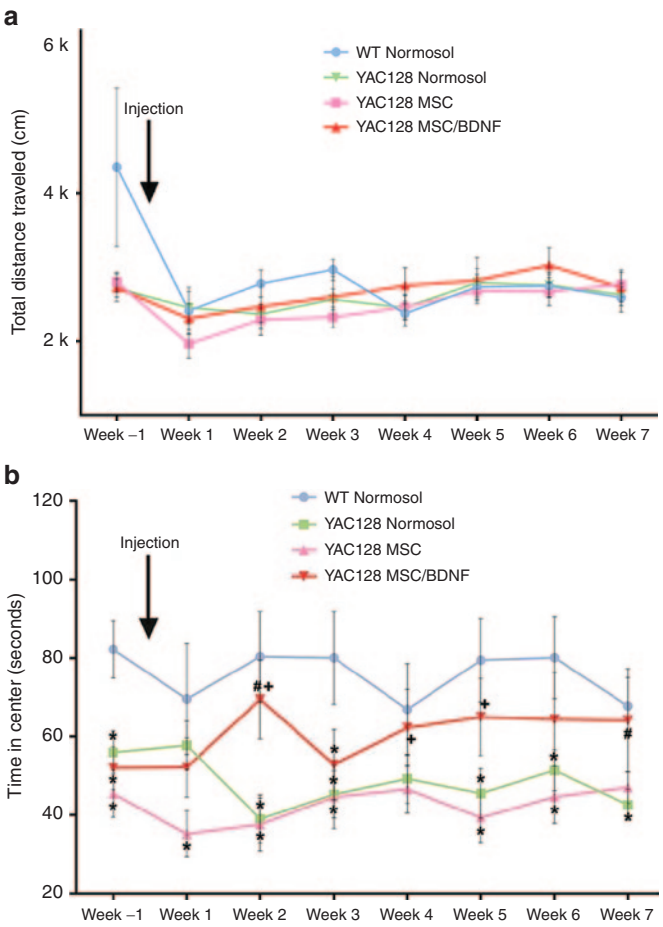

Figure 5 Open-field analysis to measure anxiety. (**a**,**b**) Each animal was placed into an open arena once a week and monitored for 10 minutes. All data was collected using Fusion system software. Total distance traveled is a measure of spontaneous exploration and is an indicator motor ability. The time in the center zone of the box was measured to test anxiety. * = Significant to WT; # = Significant to Tg + Normosol; † = Significant to Tg + MSC; $n = 16–17$/group.

MSC/BDNF efficacy: striatal volume

Following behavioral testing, mice from each of these groups were euthanized and their brains were sectioned and stained to assay striatal volume using an imaging modality. Striatal atrophy was measured by comparison to the age-matched wild type control mice, which were assigned the baseline of striatal atrophy of zero. Transplantation of MSC alone or MSC/BDNF significantly attenuated striatal atrophy (**Figure 6**). The nonmodified MSCs had an effect in reducing the striatal atrophy, to a lesser extent than MSC/BDNF. One-way ANOVA revealed no overall between-group

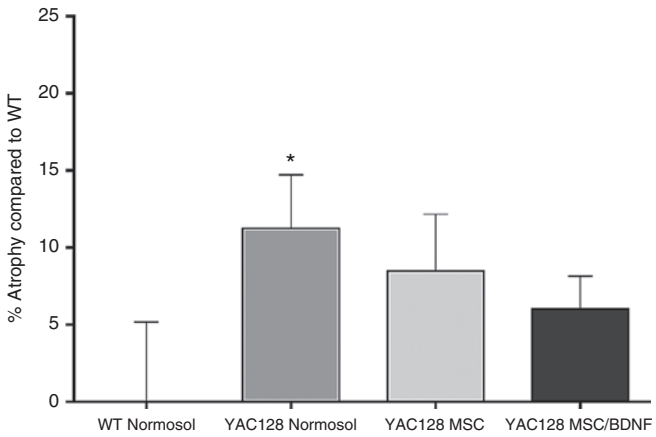

Figure 6 Striatal atrophy. Following completion of behavioral analysis in the YAC128 efficacy study, animals were euthanized and formalin perfused. Brains were cryosectioned at 30 µm and labeled with cytochrome oxidase. Brains were imaged using a Keyence BZ-9000 microscope and striatal volume was calculated using the Cavalieri principle for volume estimation. Striatal atrophy was calculated by first normalizing striatal volume to the WT group, then subtracting the value from 100. * = Significant to WT.

differences ($F(3,59) = 1.631$, $P = 0.193$). However, LSD *post hoc* analysis revealed a significant difference between WT and tg + Normosol ($P = 0.038$), but no such significant difference was observed between WT and tg + WT hMSC ($P = 0.129$) or WT and tg + BDNF hMSC ($P = 0.252$), suggesting that these cells have an intermediate effect following transplantation. A significant decrease in striatal volume was observed between vehicle treated HD mice and wild-type mice (11.2% striatal atrophy). This significant decrease in volume was not observed in the HD mice that received MSC/BDNF, which displayed only 6.03% striatal atrophy. Mice that received unmodified MSC displayed 8.47% striatal atrophy. Thus, administration of MSC/BDNF resulted in an intermediate effect, suggesting reduced striatal atrophy.

MSC/BDNF efficacy: neurogenesis

To elucidate a potential underlying mechanism of these therapeutically beneficial effects, we investigated whether neurogenesis may be increased with MSC/BDNF treatment in the R6/2 HD model. Neurogenesis assays were performed in the R6/2 mouse model of HD due to their early disease progression and very rapid decline, which more closely recapitulates the rapid progression of juvenile HD (JHD), than adult HD. The R6/2 strain only lives for 13–17 weeks in our colony, making repeated measures after immune suppression and surgery difficult. However, they are a useful strain for measuring the effects of MSC/BDNF and other agents on neurogenesis, and for examining agents that might extend lifespan.

All R6/2 mice in the study were immune suppressed using FK506/Rapamycin delivered by an Alzet osmotic pump. Mice were intrastriatally injected with vehicle, MSC or MSC/BDNF at 7 weeks of age, and euthanized at 10 weeks of age to evaluate neurogenesis. An increase in expression of an immature neuronal marker, doublecortin, was observed in the subventricular zone of the mice receiving MSC or MSC/BDNF treatment as compared to vehicle-treated controls (**Figure 7**). One-way ANOVA revealed an overall between-group differences ($F(3,26) = 5.196$, $P = 0.007$). LSD *post hoc* analysis revealed a significant difference between WT and Tg + MSC BDNF MOI 10 ($P = 0.032$), WT and Tg + MSC ($P = 0.002$), and Tg + MSC to Tg + Normosol ($P = 0.009$). A trend was observed between Tg + MSC BDNF MOI 10 and Tg + Normosol ($P = 0.121$). Taken together, this data suggests that transplantation of MSC with and without BDNF significantly increases neurogenesis activity in the subventricular zone. These data demonstrate that transplantation of MSC and MSC/BDNF leads to an increase in endogenous neurogenesis, which could potentially slow the progression of the disease.

MSC/BDNF efficacy: lifespan

Improved survival in R6/2 mice is a widely accepted and validated endpoint in this HD model. The expected lifespan, as analyzed with Kaplan-Meier, revealed that a 9.44% increase was observed in R6/2 that received WT MSC, a 7.23% increase was observed in R6/2 that received MSC BDNF MOI 10, and a 14.96% increase was observed in R6/2 that received MSC BDNF MOI 20 (**Figure 8**) as compared to Normosol-treated R6/2. These data demonstrate that MSC/BDNF treatment is neuroprotective and extends the lifespan of the R6/2 model of HD.

DISCUSSION

The current studies were performed to validate efficacy for a combined cell and gene therapy product designed to treat HD using adult human MSCs to deliver the neurotrophic factor, BDNF. Studies have shown BDNF to be an important factor in both neuronal survival and neurogenesis, making it a prime therapeutic target for neurodegenerative disorders.[27] The MSC/BDNF development candidate combines the demonstrable beneficial effects of MSC administration to the striata with the benefits of BDNF supplementation. Unlike BDNF delivery via viral vectors or recombinant protein administration into the brain, MSCs migrate into the areas of damage and independently have numerous beneficial tissue healing effects (reviewed in ref. [42]).

BDNF expression is diminished in both human HD postmortem brain as well as in HD transgenic mouse brain. In rodent

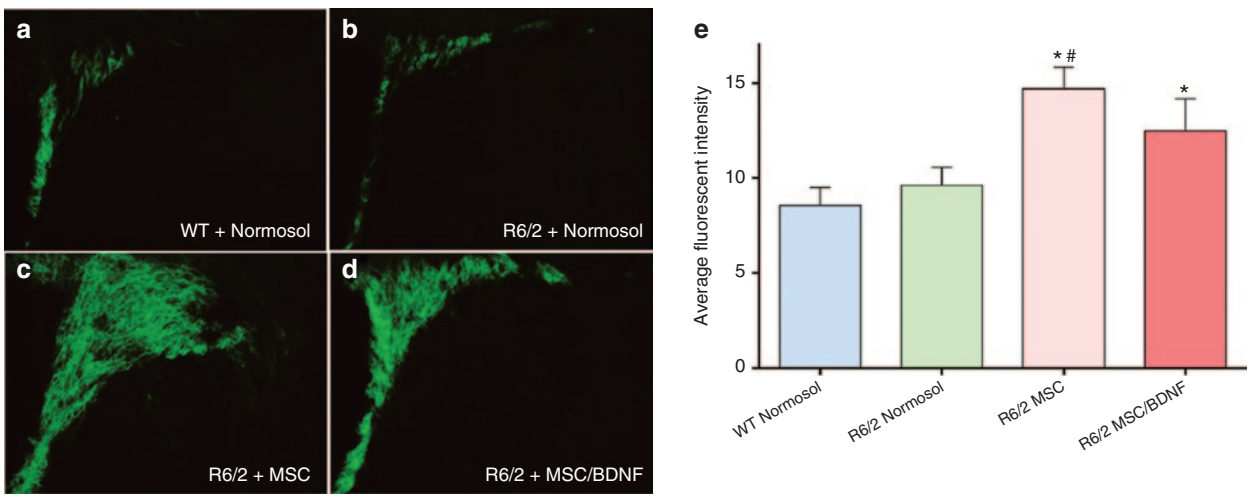

Figure 7 Neurogenesis. Three weeks following transplantation of MSC, MSC/BDNF MOI 10, or vehicle control (Normosol-R), the 10-week-old R6/2 mice were euthanized and formalin perfused. Brains were cryosectioned at 30 µm and labeled using doublecortin and AlexaFluor488. The subventricluar zone was imaged using a Zeiss Axioskop 2 microscope (10× objective) and average fluorescent intensity was calculated using ImageJ. * = Significant to WT, # = Significant to R6/2 + Normosol. *n* = 6–7/group.

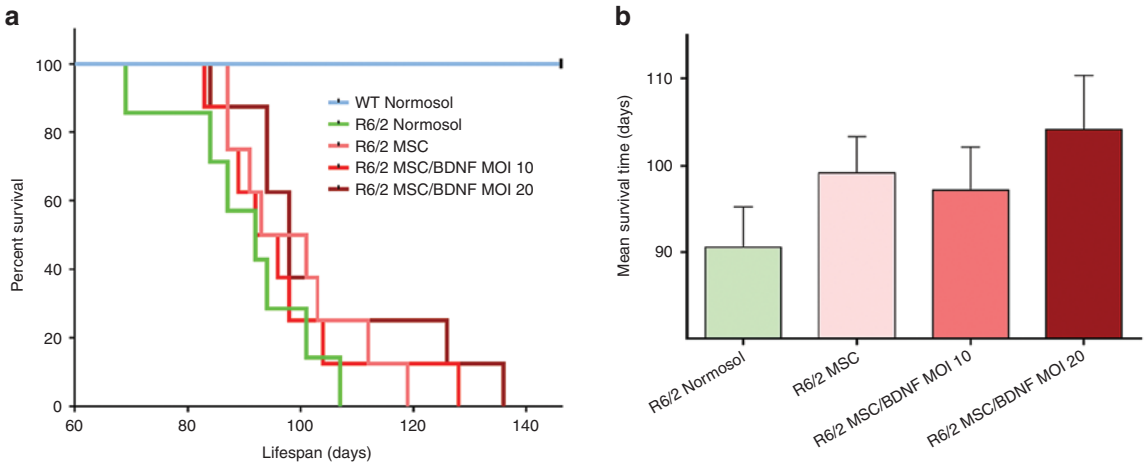

Figure 8 Implantation of MSC/BDNF increased the lifespan of R6/2 mice. Kaplan-Meier analysis: 10% increase for WT MSC, 7.7% increase for MSC/BDNF MOI 10, 15.5% increase for MSC/BDNF MOI 20. *n* = 7–9 mice per group.

models of HD, exogenous delivery of BDNF has been shown by several groups to ameliorate symptoms, attenuate the neurodegenerative process, and to extend survival.[5,9–35]

MSCs have been shown to promote endogenous neuronal growth, decrease apoptosis and regulate inflammation via the secretion of a robust profile of trophic factors. MSCs have been shown to modify the microenvironment of damaged tissue through enhanced neural regeneration and protection.[67,68] Published, peer reviewed proof of concept studies from multiple laboratories have demonstrated efficacy for MSC, BDNF, or murine MSC/BDNF cells in HD mouse models (Reviewed by Fink *et al.*[37]).

Dey *et al.*[27] demonstrated improvements in the behavioral phenotype and reduction in striatal degeneration in HD mouse models after intrastriatal administration of murine MSC/BDNF. MSCs do not permanently engraft in host tissues and generally only persist for several months. However, studies have shown that the duration of the MSC-based BDNF production should be sufficient to yield beneficial therapeutic effects in HD brains, since the neurorestorative effects of BDNF should outlast the survival of MSCs.[18,20,27,54–60] This is supported by animal data[18,20,27,54–60] and validated in the present preclinical study using human cells (MSC/BDNF).

The current preclinical studies tested whether human MSC/BDNF cells have the same therapeutic effect as seen in the previous murine studies, and were performed in two different murine models of HD: YAC128 and R6/2. The models for each primary efficacy studies were chosen due to their unique features and disease-progression as it relates to Huntington's disease. While there is no perfect animal model for HD, or any neurodegenerative disease, the YAC128 and R6/2 capture key phenotypes of the disease. The YAC128 mouse model contains the full human huntingtin gene and presents a subtle disease progression resulting in transient behavioral deficits and a slow, progressive cell loss in the striatum. The R6/2 model contains only the toxic fragment of exon 1 and displays shortened survival. The R6/2 model does not display robust neuronal loss as it is likely that the lifespan of these mice is too truncated for the neuronal dysfunction to result in a quantifiable and significant loss of cells or measurable striatal atrophy. We designed our test parameters for both the strengths and limitations of both models. For example, it would not be experimentally sound to study survival in the YAC128 as they do not exhibit a shorter lifespan than their wild-type littermates or to study the ability of the MSC to prevent neuronal loss in the R6/2 as there is no robust cell loss in the striatum. Therefore we tested neurogenesis and lifespan in the R6/2 model and behavior and striatal atrophy in the YAC128 model.

Mice were immune suppressed to allow for the extended retention of the human MSC/BDNF cells (**Figure 4**). Sham-treated and cell-treated mice were all immune suppressed and randomized between groups prior to each experiment, which were all conducted in a double-blinded manner. Importantly, in contrast to the Normosol-treated mice, the YAC128 mice treated with MSC/BDNF did *NOT* have significant levels of striatal atrophy, in comparison to wild-type mice. MSC without the additional BDNF expression had an intermediate effect. These data are important because an attenuation of striatal atrophy is the most important and definitive efficacy endpoint to be obtained in a planned future human clinical trial of MSC/BDNF.

Anxiety is a hallmark of clinical Huntington's disease and has been extensively characterized using the open field in transgenic mice and toxic lesion models of Huntington's disease. Multiple HD transgenic mouse models reveal impairments in behavior in open field testing.[18,69–74] In murine models, anxious mice spend less time in the center quadrant of an open field as anxiety increases.[18,69–74] In the current studies, there were no overall motor deficits since total distance was equivalent between groups (**Figure 5a**). However, sham-treated HD mice spent much less time in the center quadrant of the open field as compared to wild-type controls, indicating the HD mice were displaying higher levels of anxiety, as expected. This display of anxiety was significantly reduced in HD mice that were treated with MSC/BDNF (**Figure 5b**).

In the current studies, a significant increase in neurogenesis-like activity was observed in the subventricular zone in mice receiving transplantations of MSC/BDNF. MSC/BDNF treatment also resulted in a trend toward an increased lifespan of the R6/2 mice. These data suggest that MSC/BDNF could work through mechanisms of stimulating endogenous neurogenesis. Increasing

neurogenesis and striatal neuron survival is a key endpoint of a planned future clinical trial involving MSC/BDNF. Benraiss et al used adeno-associated virus (AAV) vectors to express BDNF in striatal neurons and demonstrated that AAV delivery of BDNF-induced neurogenesis and promoted a longer lifespan in a murine model of HD.[20] The observed benefit in their studies was potentiated by coexpression of noggin, which is a factor secreted by mesenchymal stem/stromal cells (MSCs).[38–41]

In the current studies conducted for efficacy, there was no evidence of weight loss or increased seizures, due to the product, no brain abnormalities observed, and no evidence of inflammation or tumor formation. No migration into spinal cord has ever been seen via luciferase. Extensive rule-out tumorigenicity studies were performed and the product is safe by these measures. No abnormal growth was ever found in the brain or other tissues of any mouse tested. Unbiased stereology showed no abnormalities, when comparing sham-injected and vehicle-injected brains. Based on the efficacy and preliminary safety data reported here, we will be performing the definitive assessments required to potentially gain FDA approval for the use of human MSC/BDNF cells in a proposed future clinical trial for HD.

Numerous clinical trials have demonstrated the biosafety of systemic infusion of allogeneic MSCs into patients with various diseases without tissue matching, as MSCs are considered relatively immune privileged (reviewed in refs. [45,75–77]). MSCs have been intracranially and intrathecally injected in previous phase 1-2 clinical trials for diseases other than HD, without adverse events.[50,53,78–82]

Additional studies of MSC injection or implantation into the CNS are ongoing or recently completed. Celgene Corporation is approved for a multi-center phase 2 clinical trial to use placenta-derived MSC for treating stroke, delivered into the brain (clinicaltrials.gov ID# NCT01310114). Placebo controlled trials for MSC injection into the CNS for TBI and stroke, as well as spinal cord injury and neurodegenerative disorders are currently ongoing (clinicaltrials.gov).[83] Athersys recently concluded patient enrollment of a phase 2a clinical study for ischemic stroke patients treated with an MSC-like stem cell therapy referred to as MultiStem. The company Brain-Storm Cell Therapeutics Inc. reported in early 2015 that it treated the first patients with amyotrophic lateral sclerosis with a genetically modified bone marrow-derived stem cell (NurOwn). No stem cell-related serious adverse events have occurred in any of these studies which provide extensive safety and provisional efficacy data for nonmatched allogeneic bone marrow-derived MSC administration to patients through FDA-approved clinical trials.

SanBio conducted a phase 1/2 gene-modified MSC clinical trial with administration into the brain to treat stroke (clinicaltrials.gov ID# NCT01287936). This clinical trial uses "next generation" gene modified cells and thus shares similarities with the proposed trial design for our MSC/BDNF product. Our proposed future clinical trial (HD-CELL) is designed to demonstrate the safety of intrastriatal implantation of gene-modified MSCs to treat HD and targets patient accrual from the ongoing observational study (PRE-CELL) at the University of California Davis (ClinicalTrials.gov study identifier NCT01937923).

Monitoring of the safety aspects of MSCs has been rigorously performed throughout these trials and no infusion or implantation-related adverse events have been reported, demonstrating the potential safety of MSC infusion into the brain when performed carefully and according to specific clinical regimens, including appropriate manufacturing processes (reviewed in Sharma *et al*. [84]).

The planned surgical techniques are based on years of previous fetal striatal implantation techniques and protocols well described by Dr. Bachoud-Levi's group in France[85–89] and Rosser and Dunnet's group in the United Kingdom.[90–93] The preclinical animal model efficacy data presented here, when coupled with *in vivo* biosafety data, supports proceeding down the FDA clinical trial pipeline. Given the strong safety record of MSCs in the clinic, our current preclinical efficacy data and the lack of effective available treatments for HD patients, we propose MSC/BDNF treatment has a favorable benefit-to-risk ratio and warrants clinical investigation.

Our stem cell-based delivery system for BDNF sets the precedent for cell-based therapy in the brain and could potentially be modified for neurodegenerative disorders such as Alzheimer's disease, Juvenile HD, ALS, spinocerebellar ataxia (SCA), and some forms of Parkinson's disease. Furthermore, this therapeutic platform provides a delivery vehicle for planned future corrective gene editing studies.

MATERIALS AND METHODS

MSC isolation and culture. Whole bone marrow was purchased commercially (All Cells, Emeryville CA). To isolate human MSCs, whole bone marrow was plated in MSC media composed of Dulbecco's modified Eagle medium—high glucose (DMEM HG), supplemented with 10% premium select fetal bovine serum (Atlanta Biologicals, Flowery Branch, GA), which was lot selected to achieve maximum growth, with additives of 1% Penicillin-streptomycin (HyClone, Marlborough, MA) and 1% L-Glutamine (HyClone). After 24 hours, nonadherent cells were discarded and adherent cells were washed twice with phosphate-buffered saline (PBS), then incubated in fresh MSC media. Cells were grown at 37 °C in 20% O_2, 5% CO_2. When MSC reached 70–80% confluence, cultures were lifted by 7 minutes of trypsinization at a concentration of 0.05% (HyClone) and reseeded at 1,000 cells/cm^2 for further subculture. Media was changed every third day.

Lentiviral production

Construction of the pCCLc-MNDU3-BDNF-WPRE vector. A cPPT fragment was cloned into the Cla-1 site downstream of the Rev-responsive element (RRE). pCCLc-X was cut with EcoRV, and the MNDU3 promoter, a modified MLV long terminal repeat promoter (that was a kind gift from Dr. Donald Kohn) cut Cla-1/Xho-1 and blunted, was cloned into this site. WPRE was cut with Cla-1, blunted, and cloned into the blunted Nhe-1 site upstream of the 3'LTR. The BDNF gene was generated via PCR of cDNA generated from RNA isolated from human bone marrow MSCs using the following primers: Forward 5′-ATG ACC ATC CTT TTC CTT ACT A-3′. Reverse: 5′-CTA TCT TCC CCT TTT AAT GGT C-3′. The BDNF was then cloned into pCR2.1 TOPO, then excised with EcoRI and cloned into the EcoRI site downstream of the MNDU3 promoter in the pCCLc-MNDU3-X-WPRE vector.

Construction of pCCLc-MNDU3-Luc-PGK-EGFP-WPRE. A blunted Cla-1 WPRE was cloned into the Sma-1 site of pCCLc-MNDU3-LUC-PGK-EGFP (gift from Dr. Donald Kohn).

Packaging. Lenti-X 293 cells (Clonetech, Mountain View, CA) were transfected with 25 μg pCCLc-MNDU3-Luc-PGK-EGFP-WPRE or pCCLc-MNDU3-BDNF-WPRE, 25 μg 8.9 packaging plasmid, and 5 μg VSVG envelope plasmid using Trans-It 293 Transfection Reagent (Mirus,

Madison, WI) in DMEM HG (HyClone). The following day, media was changed to Ultraculture Serum Free Media (Lonza, Walkersville, MD). The virus was harvested 52 hours later using Centricon Plus-70 PL-100 Filter Device (Millipore, Billerica, MA). The final product was filtered using 0.45-μm Costar Spin-X Centrifuge Filter Tubes (Millipore), aliquoted, and stored at −80 °C. Vector titer was quantified using the ABM Lentiviral qPCR Titer Kit and Evagreen Mastermix-R (abm, Richmond, BC, Canada). Replication Competency Testing was performed using the ZeptoMetrix HIV-1 p24 Antigen ELISA 2.0 Kit (ZeptoMetrix, Buffalo, NY).

Transduction. MSCs were plated at a density of 5,000 cells/cm^2. The following day, the titered lentivirus was added to the culture medium at the indicated MOI in the presence of 10 mg/ml protamine sulfate (MP Biomedical, Santa Ana, CA). After 24 hours, cells were either trypsinized and cryopreserved or the medium was replaced to allow for further culture. Transduction efficiency was determined by flow cytometry for vectors containing fluorescent markers on an FC500 (Beckman Coulter, Indianapolis, IN).

BDNF detection. Transduced cells were thawed into six-well plates (1×10^5/well), incubated in 20% O_2 for 24 hours and in 1% O_2 for an additional 48 hours. MSC media was changed to serum-free media after 24 hours in 1% O_2 and collected for ELISA after an additional 24 hours. BDNF levels were determined by ELISA (Human BDNF Quantikine ELISA, R&D Systems, Minneapolis, MN) immediately after media collection.

Vector copy number. Human MSCs were transduced with pCCLc-MNDU3-BDNF-WPRE at the indicated MOI, cryopreserved, thawed, and expanded for 3 days. DNA was isolated (Wizard Genomic DNA Purification Kit, Promega) and used for qPCR analysis. Primers/probes were designed based on published sequences and are as follows: GAPDH-5′-ACA GTC AGC CGC ATC TTC-3′ and 5′-CTC CGA CCT TCA CCT TCC-3′, WPRE—5′-TTA CGC TAT GTG GAT ACG CTG-3′, 5′-TCA TAA AGA GAC AGC AAC CAG G-3′ and 5′ /56-FAM/ AGG AGA AAA TGA AAG CCA TAC GGG AAG C /36-TAMSp/ 3′. Quantitative PCR was performed using SYBR Green PCR Master Mix (Life Technologies, Waltham, MA), TaqMan Universal PCR Master Mix, no AmpErase UNG (Life Technologies), and the indicated primers/probes under the following reaction conditions on an ABI 7300: Stage 1—50 °C for 2 minutes, Stage 2—95 °C for 10 minutes, Stage 3—40 cycles of 95 °C for 15 seconds and 60 °C for 1 minute, Stage 4 (dissociation)—95 °C for 15 seconds, 60 °C for 1 minute, 95 °C for 15 seconds, and 60 °C for 15 seconds. Quantification was based on standard curves of plasmid DNA. Vector copy number/cell was determined as WPRE/2GAPDH.

Stability of vectors in transduced cells. To determine whether there were any deletions or rearrangements in vector-transduced cells, genomic PCR was performed. Total genomic DNA was extracted from nontransduced, and BDNF vector-transduced MSC using the Quick gDNA MiniPrep kit (Zymo Research, Irvine, CA). PCR was performed using high-fidelity Taq (Affymetrix, Santa Clara, CA). Primers corresponding to the specific vector transgenes were used: ψ (forward) 5′-ACCTGAAAGCGAAAGGGAAAC-3′, U5-3′ (reverse) 5′-CTGCTAGAGATTTTCCACACTGAC-3′, MNDU3 (forward) 5′-CGCCCT CAGCAGTTTCTAG-3′, MNDU3 (reverse) 5′-CTATCT ATGGCTCGTACTCTATA-3′, BDNF (forward) 5′-CCATAAGGACGC GGACTTGTA-3′, and BDNF (reverse) 5′-GAGGAGGCTCCAAAGG CACTT-3′. PCR products were analyzed and visualized on an agarose gel.

MSC lineage differentiation. MSCs were differentiated into an osteogenic lineage by plating at approximately 10,000 cells/cm^2 and culturing for 16 days in DMEM HG containing 10% fetal bovine serum (FBS), 1× L-glutamine, 0.2 mmol/l ascorbic acid, 0.1 μmol/l dexamethasone, and 10 mmol/l β-glycerophosphate with medium changes every 2 days. For adipogenic differentiation, MSC were plated at approximately 10,000 cells/cm^2 and cultured for 16 days in DMEM HG containing 10% FBS, 1× L-glutamine, 0.5 mmol/l isobutylmethyxanthine, 50 μmol/l indomethacin, and 0.5 μmol/l dexamethosone with medium changes every 2 days (Ogawa *et al.*[94]). Plates were washed with PBS (+Calcium/+Magnesium), fixed in formalin for 5 minutes, washed, then stained with Alizarin Red S Indicator (RICCA, Arlington, TX) or Oil red O Solution (Electron Microscopy Sciences, Hatfield, PA) for 5 minutes. Plates were then washed for image analysis using a 10× objective on a Nikon Eclipse microscope.

Cell proliferation. MSCs were plated at approximately 1,000 cells/cm^2 in 24-well plates and cultured as described. After 1, 3, 5, 7, and 9 days in culture, plates were analyzed using CellTiter96 Non-radioactive Cell Proliferation Assay (Promega, Madison, WI), following the manufacturer's protocol. MTT dye solution was added directly to culture medium. The plate was returned to the incubator for 2 hours before halting the reaction with stop solution. Samples were stored at 4 °C until completion of the time course, at which time the plates were returned to 37 °C for 2 hours until the dye crystals had fully dissolved. Then, 100 μl from each well was loaded into a 96-well plate, which was analyzed for absorbance at 570 nm with a reference at 650 nm on a microplate spectrometer (Emax, Molecular Devices, Sunnyvale, CA). The number of cells was calculated from a standard curve generated from known numbers of cells treated identically to the above using a linear regression.

In vivo *imaging study.* Whole bone marrow was purchased commercially (Lonza, Walkersville, MD) and MSCs were isolated, transduced, and expanded as described.[95] Immune-competent FVB/NJ (Friend Virus B NIH Jackson) mice and immune-deficient NSG (NOD SCID γ-/-) mice bred in-house were used for this study at 4 months of age. Human MSCs were transduced by a lentiviral vector carrying the luciferase gene (pCCLc-MNDU3-Luc-PGK-EGFP-WPRE), which allows cells to be visualized in the brains of living mice over time (MSC-Luc). FVB/NJ animals (3M/2F) were assigned to the following groups: noninjected (imaging control), MSC-Luc or MSC-Luc + Immune suppression (FK506/Rapamycin delivered by Alzet osmotic pump as described below). Additionally, immune-deficient NSG mice (3M/2F) were injected with MSC-Luc as positive controls. Unilateral striatal implantation of passage 5 MSCs was performed as described above (2.5×10^5 cells in the left hemisphere).

Bioluminescence was detected in anesthetized animals via IVIS Spectrum (Perkin Elmer, Waltham, MA) (Perkin Elmer) 15 minutes postintraperitoneal luciferin injection (3 mg/mouse, XenoLight D-Luciferin K+ Salt, Perkin Elmer). Mice were imaged on post-op days 2, 4, 7, 9, 11, 14, and then weekly for 5 weeks. Animals used in this study were housed under normal 12-hour light/12-hour dark cycle conditions. All procedures were reviewed and approved by the UC Davis Institutional Animal Care and Use Committee (IACUC).

Animals. YAC128: YAC128 mice (Jackson Labs stock #004938, Bar Harbor, ME) were immune suppressed by receiving FK506 and Rapamycin (1 μg/g/day each) by Alzet osmotic pumps (Model 1004, Alzet Osmotic Pumps, Cupertino, CA) implanted subcutaneously four days prior to cell implantation. Pumps were preloaded with FK506/Rapa diluted in 50%DMSO/50%PEG and incubated in Normosol-R @ 37 °C × 48 hours prior to implantation. FK506 (Tacrolimus) and Rapamycin (Sirolimus) were purchased from InVivoGen, San Diego, CA. Mice were implanted bilaterally into the striata with vehicle, MSC or MSC/BDNF MOI 10 at 8 ½ months of age. Mice received 5×10^5 cells (passage 6) per hemisphere in 5 μl vehicle. Behavioral data was collected weekly following cell implantation until 10 months of age (initial behavioral training and testing began at 4 ½ months). At 10 months of age, animals were euthanized and brains were collected for histological analysis. This study was run in two cohorts and data was combined for statistical analysis.

R6/2: R6/2 120CAG (Jackson Labs stock #006494) mice were immune suppressed using FK506/Rapamycin delivered by an Alzet osmotic pump as described above. Mice were bilaterally implanted into the striata with vehicle, MSC, MSC/BDNF MOI 10 or MSC/BDNF MOI 20 at 7 weeks

of age. Mice received 5×10^5 cells (passage 6) per hemisphere in 5 µl vehicle. Behavioral testing began at 6 weeks of age and continued weekly following cell implantation. Mice were sacrificed 3 weeks following cell implantation in order to process the brains for histology. An additional cohort of nonimmune-suppressed animals was used to collect survival data following the UC Davis IACUC guidelines on humane endpoints.

All mice were individually housed on a reverse light cycle with food and water *ad libitum* for the duration of the study. All procedures were reviewed and approved by the UC Davis IACUC.

Surgical procedures and monitoring. All surgical procedures were conducted in compliance with the UC Davis IACUC policy on rodent survival surgery.

Alzet pump implantation. Prior to surgery, hair was removed using a depilatory. Animals were anesthetized using isoflurane (2–3% in oxygen). Skin was cleaned with betadine and wiped clean with an alcohol pad. Alzet pumps (Model 1004, Alzet Osmotic Pumps, Cupertino, CA) were implanted subcutaneously through a small incision between the scapulae with the flow moderator portion of the pump pointing away from the incision. The skin incision was then closed with 6-0 silk suture.

Cell preparation. Prior to surgery, cells were thawed and incubated at 37 °C in 20% O_2, 5% CO_2 for 24 hours. Subsequently, the media was changed and cells were further incubated at 37°C in 1% O_2, 5% CO_2 for an additional 48 hours prior to implantation as previously described.[96,97]

Cell implantation. Prior to surgery, hair was removed from the head using Nair. Animals were anesthetized using isoflurane (2–3% in oxygen) and placed into a stereotaxic frame. Skin was then cleaned with betadine and wiped clean with an alcohol pad. A small incision was made in the scalp to allow visualization of the skull. A small (1 mm) burr hole was made in the skull at 0.5 mm AP and ±2.0 mm ML relative to bregma. Cells were injected into the striatum at a depth of 2.5 mm using a Hamilton syringe at a rate of 0.5 µl/minute in a total volume of 5 µl. After waiting an additional 5 minutes after injection, the syringe was slowly removed, the burr holes were filled with bone wax and the incision sutured with 6-0 silk suture.

Pain management. Carprofen (5 mg/kg) was administered by subcutaneous injection at the time of surgery and again the following day. All postoperative animals were observed daily for 7 days in order to monitor recovery and incision healing.

Open field. Each animal was placed into the center of an open arena once a week and monitored for 10 minutes. All data was collected using Fusion system software. Technicians performing the assays were blinded to implantation group in all studies.

Histology. Following completion of behavioral analysis, animals were sacrificed and transcardially perfused with saline solution followed by formalin (PROTOCOL, Kalamazoo, MI). Brains were harvested, weighed, fixed in formalin at room temperature for 24 hours, transferred to a 30% sucrose solution at 4 °C for 24–48 hours then cryopreserved by submersion in dry ice cooled isopropyl alcohol for 5 minutes. Brains were then wrapped in foil and stored at −80 °C. Brains were prewarmed to −20 °C and cryosectioned at 30 µm.

For analysis of endogenous neurogenesis occurring in the subventricular zone in response to the MSC transplantation, the tissue was labeled with anti-Doublecortin (rabbit Doublecortin; 1/500, Abcam 18723, Cambridge, MA), a label of immature neurons. The tissue was incubated in blocking solution for 45 minutes at room temperature (blocking solution: 2% normal goat serum, 1% bovine serum albumin, 0.1% Triton-X, 0.05% Tween-20 in 0.01M PBS). The tissue was then transferred to a well containing the primary antibody and stored at 4 °C overnight with gentle agitation. The following day, the tissue was rinsed three times in PBS and transferred to a well containing anti-rabbit AlexaFluor488 (1/300; Invitrogen, Grand Island, NY) for 1 hour at room temperature and given gentle agitation. The tissue was then rinsed three times in PBS and coverslipped using Fluoromount (Sigma, St. Louis, MO).

Cytochrome oxidase histology was used to delineate structures in the brain and was used for volumetric analysis. The tissue was submersed in a solution of 800 mg sucrose, 4 mg of cytochrome C (Calbiochem, Billerica, MA), and 1 mg of 3,3′-Diaminobenzidine tetrahydrochloride (Sigma) dissolved in 20 ml of PBS for 4 hours at room temperature with gentle agitation. The tissue was then transferred to deionized H_2O, mounted onto positively charged glass slides, and coverslipped using Permount (Fisher, Waltham, MA).

Image acquisition and analysis. Images of the fluorescent labels were captured using a Zeiss Axiskop 2 *plus* fluorescent microscope at 10× magnification. Cytochrome oxidase-labeled tissue was imaged using a Keyence BZ-9000 at 4× and then images were stitched together using Keyence viewer software. Images were captured from nine levels, centered at the transplant site with additional sections anterior and posterior to the transplant site, approximately 180 µm apart.

All images were analyzed using ImageJ (NIH, Bethesda, MD). Average intensity of doublecortin was measured in the subventricular zone of each group. Striatal volume was calculated using Cavalieri's volume estimation.

Statistics. All statistical analyses were performed using SPSS v22 with an α-level equal to 0.05. All behavioral data was analyzed using a repeated measures ANOVA to measure changes between genotypes and treatments across weeks. Histological data was analyzed using a one-way ANOVA. When appropriate, a LSD *post hoc* was performed. Survival was analyzed using Kaplan-Meier analysis.

ACKNOWLEDGMENTS

This work was supported by the California Institute for Regenerative Medicine (CIRM DR2-05415) (V.W./J.A.N.), National Institute of Health Director's transformative award (R01GM099688) (J.A.N.), training programs NSF GRFP 2011116000, NIH T32-GM008799, NSF GROW 201111600, T32-HL086350 (J.D.A.), the CIRM Bridges training program TB1-01184 (H.D. and H.N.), a National Institute of Health National Research Service Award Postdoctoral Fellowship F32NS090722 (K.D.F.), a gift from the Stewart's and Dake Family (J.A.N./K.D.F.), and philanthropic donors from the HD community, including the Roberson family and Team KJ. The authors declared no conflict of interest.

REFERENCES

1. A novel gene containing a trinucleotide repeat that is expanded and unstable on Huntington's disease chromosomes. The Huntington's Disease Collaborative Research Group. *Cell* **72**: 971–983 (1993).
2. Huntington Study, G (2006). Tetrabenazine as antichorea therapy in Huntington disease: a randomized controlled trial. *Neurology* **66**: 366–372.
3. Killoran, A and Biglan, KM (2014). Current therapeutic options for Huntington's disease: good clinical practice versus evidence-based approaches? *Mov Disord* **29**: 1404–1413.
4. Scheuing, L, Chiu, CT, Liao, HM, Linares, GR and Chuang, DM (2014). Preclinical and clinical investigations of mood stabilizers for Huntington's disease: what have we learned? *Int J Biol Sci* **10**: 1024–1038.
5. Canals, JM, Pineda, JR, Torres-Peraza, JF, Bosch, M, Martín-Ibañez, R, Muñoz, MT *et al.* (2004). Brain-derived neurotrophic factor regulates the onset and severity of motor dysfunction associated with enkephalinergic neuronal degeneration in Huntington's disease. *J Neurosci* **24**: 7727–7739.
6. Her, LS and Goldstein, LS (2008). Enhanced sensitivity of striatal neurons to axonal transport defects induced by mutant huntingtin. *J Neurosci* **28**: 13662–13672.
7. Wu, LL, Fan, Y, Li, S, Li, XJ and Zhou, XF (2010). Huntingtin-associated protein-1 interacts with pro-brain-derived neurotrophic factor and mediates its transport and release. *J Biol Chem* **285**: 5614–5623.
8. Antoniades, CA and Watts, C (2013). Huntington's disease and cell therapies: past, present, and future. *Methods Mol Biol* **1010**: 19–32.
9. Torres-Peraza, JF, Giralt, A, García-Martínez, JM, Pedrosa, E, Canals, JM and Alberch, J (2008). Disruption of striatal glutamatergic transmission induced by mutant huntingtin involves remodeling of both postsynaptic density and NMDA receptor signaling. *Neurobiol Dis* **29**: 409–421.
10. Conforti, P, Ramos, C, Apostol, BL, Simmons, DA, Nguyen, HP, Riess, O *et al.* (2008). Blood level of brain-derived neurotrophic factor mRNA is progressively reduced in rodent models of Huntington's disease: restoration by the neuroprotective compound CEP-1347. *Mol Cell Neurosci* **39**: 1–7.
11. Zuccato, C, Belyaev, N, Conforti, P, Ooi, L, Tartari, M, Papadimou, E *et al.* (2007). Widespread disruption of repressor element-1 silencing transcription factor/neuron-restrictive silencer factor occupancy at its target genes in Huntington's disease. *J Neurosci* **27**: 6972–6983.

12. Ciammola, A, Sassone, J, Cannella, M, Calza, S, Poletti, B, Frati, L *et al.* (2007). Low brain-derived neurotrophic factor (BDNF) levels in serum of Huntington's disease patients. *Am J Med Genet B Neuropsychiatr Genet* **144B**: 574–577.
13. Zuccato, C, Liber, D, Ramos, C, Tarditi, A, Rigamonti, D, Tartari, M *et al.* (2005). Progressive loss of BDNF in a mouse model of Huntington's disease and rescue by BDNF delivery. *Pharmacol Res* **52**: 133–139.
14. Zuccato, C, Ciammola, A, Rigamonti, D, Leavitt, BR, Goffredo, D, Conti, L *et al.* (2001). Loss of huntingtin-mediated BDNF gene transcription in Huntington's disease. *Science* **293**: 493–498.
15. Serrano Sánchez, T, Alberti Amador, E, Lorigados Pedre, L, Blanco Lezcano, L, Diaz Armesto, I and Bergado, JA (2014). BDNF in quinolinic acid lesioned rats after bone marrow cells transplant. *Neurosci Lett* **559**: 147–151.
16. Samadi, P, Boutet, A, Rymar, VV, Rawal, K, Maheux, J, Kvann, JC *et al.* (2013). Relationship between BDNF expression in major striatal afferents, striatum morphology and motor behavior in the R6/2 mouse model of Huntington's disease. *Genes Brain Behav* **12**: 108–124.
17. Martire, A, Pepponi, R, Domenici, MR, Ferrante, A, Chiodi, V and Popoli, P (2013). BDNF prevents NMDA-induced toxicity in models of Huntington's disease: the effects are genotype specific and adenosine A2A receptor is involved. *J Neurochem* **125**: 225–235.
18. Giampà, C, Montagna, E, Dato, C, Melone, MA, Bernardi, G and Fusco, FR (2013). Systemic delivery of recombinant brain derived neurotrophic factor (BDNF) in the R6/2 mouse model of Huntington's disease. *PLoS One* **8**: e64037.
19. Reiner, A, Wang, HB, Del Mar, N, Sakata, K, Yoo, W and Deng, YP (2012). BDNF may play a differential role in the protective effect of the mGluR2/3 agonist LY379268 on striatal projection neurons in R6/2 Huntington's disease mice. *Brain Res* **1473**: 161–172.
20. Benraiss, A, Bruel-Jungerman, E, Lu, G, Economides, AN, Davidson, B and Goldman, SA (2012). Sustained induction of neuronal addition to the adult rat neostriatum by AAV4-delivered noggin and BDNF. *Gene Ther* **19**: 483–493.
21. Giralt, A, Carretón, O, Lao-Peregrin, C, Martín, ED and Alberch, J (2011). Conditional BDNF release under pathological conditions improves Huntington's disease pathology by delaying neuronal dysfunction. *Mol Neurodegener* **6**: 71.
22. Arregui, L, Benítez, JA, Razgado, LF, Vergara, P and Segovia, J (2011). Adenoviral astrocyte-specific expression of BDNF in the striata of mice transgenic for Huntington's disease delays the onset of the motor phenotype. *Cell Mol Neurobiol* **31**: 1229–1243.
23. Zajac, MS, Pang, TY, Wong, N, Weinrich, B, Leang, LS, Craig, JM *et al.* (2010). Wheel running and environmental enrichment differentially modify exon-specific BDNF expression in the hippocampus of wild-type and pre-motor symptomatic male and female Huntington's disease mice. *Hippocampus* **20**: 621–636.
24. Xie, Y, Hayden, MR and Xu, B (2010). BDNF overexpression in the forebrain rescues Huntington's disease phenotypes in YAC128 mice. *J Neurosci* **30**: 14708–14718.
25. Saylor, AJ and McGinty, JF (2010). An intrastriatal brain-derived neurotrophic factor infusion restores striatal gene expression in Bdnf heterozygous mice. *Brain Struct Funct* **215**: 97–104.
26. Giralt, A, Friedman, HC, Caneda-Ferrón, B, Urbán, N, Moreno, E, Rubio, N *et al.* (2010). BDNF regulation under GFAP promoter provides engineered astrocytes as a new approach for long-term protection in Huntington's disease. *Gene Ther* **17**: 1294–1308.
27. Dey, ND, Bombard, MC, Roland, BP, Davidson, S, Lu, M, Rossignol, J *et al.* (2010). Genetically engineered mesenchymal stem cells reduce behavioral deficits in the YAC 128 mouse model of Huntington's disease. *Behav Brain Res* **214**: 193–200.
28. Wu, CL, Hwang, CS and Yang, DI (2009). Protective effects of brain-derived neurotrophic factor against neurotoxicity of 3-nitropropionic acid in rat cortical neurons. *Neurotoxicology* **30**: 718–726.
29. Simmons, DA, Rex, CS, Palmer, L, Pandyarajan, V, Fedulov, V, Gall, CM *et al.* (2009). Up-regulating BDNF with an ampakine rescues synaptic plasticity and memory in Huntington's disease knockin mice. *Proc Natl Acad Sci USA* **106**: 4906–4911.
30. Giralt, A, Rodrigo, T, Martín, ED, Gonzalez, JR, Milà, M, Ceña, V *et al.* (2009). Brain-derived neurotrophic factor modulates the severity of cognitive alterations induced by mutant huntingtin: involvement of phospholipaseCgamma activity and glutamate receptor expression. *Neuroscience* **158**: 1234–1250.
31. Kells, AP, Henry, RA and Connor, B (2008). AAV-BDNF mediated attenuation of quinolinic acid-induced neuropathology and motor function impairment. *Gene Ther* **15**: 966–977.
32. Gharami, K, Xie, Y, An, JJ, Tonegawa, S and Xu, B (2008). Brain-derived neurotrophic factor over-expression in the forebrain ameliorates Huntington's disease phenotypes in mice. *J Neurochem* **105**: 369–379.
33. Lynch, G, Kramar, EA, Rex, CS, Jia, Y, Chappas, D, Gall, CM *et al.* (2007). Brain-derived neurotrophic factor restores synaptic plasticity in a knock-in mouse model of Huntington's disease. *J Neurosci* **27**: 4424–4434.
34. Pérez-Navarro, E, Canudas, AM, Akerund, P, Alberch, J and Arenas, E (2000). Brain-derived neurotrophic factor, neurotrophin-3, and neurotrophin-4/5 prevent the death of striatal projection neurons in a rodent model of Huntington's disease. *J Neurochem* **75**: 2190–2199.
35. Martínez-Serrano, A and Björklund, A (1996). Protection of the neostriatum against excitotoxic damage by neurotrophin-producing, genetically modified neural stem cells. *J Neurosci* **16**: 4604–4616.
36. Alberch, J, Pérez-Navarro, E and Canals, JM (2004). Neurotrophic factors in Huntington's disease. *Prog Brain Res* **146**: 195–229.
37. Fink KD, Deng, P, Torrest, A, Stewart H, Pollock K, Gruenloh W *et al.* (2015). Developing stem cell therapies for Juvenile and adult onset Huntington's disease. *Regen Med* **10**: 623–646.
38. Heliotis, M and Tsiridis, E (2008). Suppression of bone morphogenetic protein inhibitors promotes osteogenic differentiation: therapeutic implications. *Arthritis Res Ther* **10**: 115.
39. Wan, DC, Pomerantz, JH, Brunet, LJ, Kim, JB, Chou, YF, Wu, BM *et al.* (2007). Noggin suppression enhances *in vitro* osteogenesis and accelerates *in vivo* bone formation. *J Biol Chem* **282**: 26450–26459.
40. Levi, B, Nelson, ER, Hyun, JS, Glotzbach, JP, Li, S, Nauta, A *et al.* (2012). Enhancement of human adipose-derived stromal cell angiogenesis through knockdown of a BMP-2 inhibitor. *Plast Reconstr Surg* **129**: 53–66.
41. Chen, C, Uludağ, H, Wang, Z and Jiang, H (2012). Noggin suppression decreases BMP-2-induced osteogenesis of human bone marrow-derived mesenchymal stem cells *in vitro*. *J Cell Biochem* **113**: 3672–3680.
42. Olson, SD, Pollock, K, Kambal, A, Cary, W, Mitchell, GM, Tempkin, J *et al.* (2012). Genetically engineered mesenchymal stem cells as a proposed therapeutic for Huntington's disease. *Mol Neurobiol* **45**: 87–98.
43. Meyerrose, T *et al. Establishment and Transduction of Primary Human Stromal/ Mesenchymal Stem Cell Monolayers*. Chapter 2. Kluwer Academic Publishers, 2006.
44. Meyerrose, T, Olson, S, Pontow, S, Kalomoiris, S, Jung, Y, Annett, G *et al.* (2010). Mesenchymal stem cells for the sustained *in vivo* delivery of bioactive factors. *Adv Drug Deliv Rev* **62**: 1167–1174.
45. Murphy, MB, Moncivais, K and Caplan, AI (2013). Mesenchymal stem cells: environmentally responsive therapeutics for regenerative medicine. *Exp Mol Med* **45**: e54.
46. Mendonça, MV, Larocca, TF, de Freitas Souza, BS, Villarreal, CF, Silva, LF, Matos, AC *et al.* (2014). Safety and neurological assessments after autologous transplantation of bone marrow mesenchymal stem cells in subjects with chronic spinal cord injury. *Stem Cell Res Ther* **5**: 126.
47. Newell, LF, Deans, RJ and Maziarz, RT (2014). Adult adherent stromal cells in the management of graft-versus-host disease. *Expert Opin Biol Ther* **14**: 231–246.
48. Lunn, JS, Sakowski, SA and Feldman, EL (2014). Concise review: Stem cell therapies for amyotrophic lateral sclerosis: recent advances and prospects for the future. *Stem Cells* **32**: 1099–1109.
49. Lalu, MM, Moher, D, Marshall, J, Fergusson, D, Mei, SH, Macleod, M *et al.*; Canadian Critical Care Translational Biology Group. (2014). Efficacy and safety of mesenchymal stromal cells in preclinical models of acute lung injury: a systematic review protocol. *Syst Rev* **3**: 48.
50. Aleynik, A, Gernavage, KM, Mourad, YSh, Sherman, LS, Liu, K, Gubenko, YA *et al.* (2014). Stem cell delivery of therapies for brain disorders. *Clin Transl Med* **3**: 24.
51. Munir, H and McGettrick, HM (2015). Mesenchymal stem cell therapy for autoimmune disease: risks and rewards. *Stem Cells Dev* **24**: 2091–2100.
52. Uth, K and Trifonov, D (2014). Stem cell application for osteoarthritis in the knee joint: A minireview. *World J Stem Cells* **6**: 629–636.
53. Ng, TK, Fortino, VR, Pelaez, D and Cheung, HS (2014). Progress of mesenchymal stem cell therapy for neural and retinal diseases. *World J Stem Cells* **6**: 111–119.
54. Benraiss, A and Goldman, SA (2011). Cellular therapy and induced neuronal replacement for Huntington's disease. *Neurotherapeutics* **8**: 577–590.
55. Benraiss, A, Toner, MJ, Xu, Q, Bruel-Jungerman, E, Rogers, EH, Wang, F *et al.* (2013). Sustained mobilization of endogenous neural progenitors delays disease progression in a transgenic model of Huntington's disease. *Cell Stem Cell* **12**: 787–799.
56. Rossignol, J, Fink, K, Davis, K, Clerc, S, Crane, A, Matchynski, J *et al.* (2014). Transplants of adult mesenchymal and neural stem cells provide neuroprotection and behavioral sparing in a transgenic rat model of Huntington's disease. *Stem Cells* **32**: 500–509.
57. Rossignol, J, Boyer, C, Lévèque, X, Fink, KD, Thinard, R, Blanchard, F *et al.* (2011). Mesenchymal stem cell transplantation and DMEM administration in a 3NP rat model of Huntington's disease: morphological and behavioral outcomes. *Behav Brain Res* **217**: 369–378.
58. Lescaudron, L, Unni, D and Dunbar, GL (2003). Autologous adult bone marrow stem cell transplantation in an animal model of huntington's disease: behavioral and morphological outcomes. *Int J Neurosci* **113**: 945–956.
59. Edalatmanesh, MA, Matin, MM, Neshati, Z, Bahrami, AR and Kheirabadi, M (2010). Systemic transplantation of mesenchymal stem cells can reduce cognitive and motor deficits in rats with unilateral lesions of the neostriatum. *Neurol Res* **32**: 166–172.
60. Snyder, BR, Chiu, AM, Prockop, DJ and Chan, AW (2010). Human multipotent stromal cells (MSCs) increase neurogenesis and decrease atrophy of the striatum in a transgenic mouse model for Huntington's disease. *PLoS One* **5**: e9347.
61. Dull, T, Zufferey, R, Kelly, M, Mandel, RJ, Nguyen, M, Trono, D *et al.* (1998). A third-generation lentivirus vector with a conditional packaging system. *J Virol* **72**: 8463–8471.
62. Challita, PM, Skelton, D, el-Khoueiry, A, Yu, XJ, Weinberg, K and Kohn, DB (1995). Multiple modifications in cis elements of the long terminal repeat of retroviral vectors lead to increased expression and decreased DNA methylation in embryonic carcinoma cells. *J Virol* **69**: 748–755.
63. Candotti, F, Shaw, KL, Muul, L, Carbonaro, D, Sokolic, R, Choi, C *et al.* (2012). Gene therapy for adenosine deaminase-deficient severe combined immune deficiency: clinical comparison of retroviral vectors and treatment plans. *Blood* **120**: 3635–3646.
64. Folstein, SE (1991). The psychopathology of Huntington's disease. *Res Publ Assoc Res Nerv Ment Dis* **69**: 181–191.
65. Anderson, KE and Marder, KS (2001). An overview of psychiatric symptoms in Huntington's disease. *Curr Psychiatry Rep* **3**: 379–388.
66. Craufurd, D, Thompson, JC and Snowden, JS (2001). Behavioral changes in Huntington Disease. *Neuropsychiatry Neuropsychol Behav Neurol* **14**: 219–226.
67. Crigler, L, Robey, RC, Asawachaicharn, A, Gaupp, D and Phinney, DG (2006). Human mesenchymal stem cell subpopulations express a variety of neuro-regulatory molecules and promote neuronal cell survival and neuritogenesis. *Exp Neurol* **198**: 54–64.
68. Kassis, I, Grigoriadis, N, Gowda-Kurkalli, B, Mizrachi-Kol, R, Ben-Hur, T, Slavin, S *et al.* (2008). Neuroprotection and immunomodulation with mesenchymal stem cells in chronic experimental autoimmune encephalomyelitis. *Arch Neurol* **65**: 753–761.
69. Berry, SE (2015). Concise review: mesoangioblast and mesenchymal stem cell therapy for muscular dystrophy: progress, challenges, and future directions. *Stem Cells Transl Med* **4**: 91–98.
70. Moll, G, Alm, JJ, Davies, LC, von Bahr, L, Heldring, N, Stenbeck-Funke, L *et al.* (2014). Do cryopreserved mesenchymal stromal cells display impaired immunomodulatory and therapeutic properties? *Stem Cells* **32**: 2430–2442.

71. Kingsman, SM, Mitrophanous, K and Olsen, JC (2005). Potential oncogene activity of the woodchuck hepatitis post-transcriptional regulatory element (WPRE). *Gene Ther* **12**: 3–4.
72. Rattray, I, Smith, EJ, Crum, WR, Walker, TA, Gale, R, Bates, GP *et al.* (2013). Correlations of behavioral deficits with brain pathology assessed through longitudinal MRI and histopathology in the R6/1 mouse model of Huntington's disease. *PLoS One* **8**: e84726.
73. Southwell, AL, Franciosi, S, Villanueva, EB, Xie, Y, Winter, LA, Veeraraghavan, J *et al.* (2015). Anti-semaphorin 4D immunotherapy ameliorates neuropathology and some cognitive impairment in the YAC128 mouse model of Huntington disease. *Neurobiol Dis* **76**: 46–56.
74. Southwell, AL, Warby, SC, Carroll, JB, Doty, CN, Skotte, NH, Zhang, W *et al.* (2013). A fully humanized transgenic mouse model of Huntington disease. *Hum Mol Genet* **22**: 18–34.
75. Sokal, EM, Lombard, C and Mazza, G (2015). Mesenchymal stem cell treatment for hemophilia: a review of current knowledge. *J Thromb Haemost* **13 Suppl 1**: S161–S166.
76. Nordberg, RC and Loboa, EG (2015). Our fat future: translating adipose stem cell therapy. *Stem Cells Transl Med* **4**: 974–979.
77. Luk, F, de Witte, SF, Bramer, WM, Baan, CC and Hoogduijn, MJ (2015). Efficacy of immunotherapy with mesenchymal stem cells in man: a systematic review. *Expert Rev Clin Immunol* **11**: 617–636.
78. Zhang, ZX, Guan, LX, Zhang, K, Zhang, Q and Dai, LJ (2008). A combined procedure to deliver autologous mesenchymal stromal cells to patients with traumatic brain injury. *Cytotherapy* **10**: 134–139.
79. Díez-Tejedor, E, Gutiérrez-Fernández, M, Martínez-Sánchez, P, Rodríguez-Frutos, B, Ruiz-Ares, G, Lara, ML *et al.* (2014). Reparative therapy for acute ischemic stroke with allogeneic mesenchymal stem cells from adipose tissue: a safety assessment: a phase II randomized, double-blind, placebo-controlled, single-center, pilot clinical trial. *J Stroke Cerebrovasc Dis* **23**: 2694–2700.
80. Haidet-Phillips, AM and Maragakis, NJ (2015). Neural and glial progenitor transplantation as a neuroprotective strategy for amyotrophic lateral sclerosis (ALS). *Brain Res* **1628**(Pt B): 343–350.
81. Thomsen, GM, Gowing, G, Svendsen, S and Svendsen, CN (2014). The past, present and future of stem cell clinical trials for ALS. *Exp Neurol* **262 Pt B**: 127–137.
82. Faravelli, I, Riboldi, G, Nizzardo, M, Simone, C, Zanetta, C, Bresolin, N *et al.* (2014). Stem cell transplantation for amyotrophic lateral sclerosis: therapeutic potential and perspectives on clinical translation. *Cell Mol Life Sci* **71**: 3257–3268.
83. Venkataramana, NK, Kumar, SK, Balaraju, S, Radhakrishnan, RC, Bansal, A, Dixit, A *et al.* (2010). Open-labeled study of unilateral autologous bone-marrow-derived mesenchymal stem cell transplantation in Parkinson's disease. *Transl Res* **155**: 62–70.
84. Sharma, RR, Pollock, K, Hubel, A and McKenna, D (2014). Mesenchymal stem or stromal cells: a review of clinical applications and manufacturing practices. *Transfusion* **54**: 1418–1437.
85. Bachoud-Lévi, AC (2009). Neural grafts in Huntington's disease: viability after 10 years. *Lancet Neurol* **8**: 979–981.
86. Bachoud-Lévi, AC, Déglon, N, Nguyen, JP, Bloch, J, Bourdet, C, Winkel, L *et al.* (2000). Neuroprotective gene therapy for Huntington's disease using a polymer encapsulated BHK cell line engineered to secrete human CNTF. *Hum Gene Ther* **11**: 1723–1729.
87. Bachoud-Lévi, AC, Gaura, V, Brugières, P, Lefaucheur, JP, Boissé, MF, Maison, P *et al.* (2006). Effect of fetal neural transplants in patients with Huntington's disease 6 years after surgery: a long-term follow-up study. *Lancet Neurol* **5**: 303–309.
88. Bachoud-Lévi, AC, Rémy, P, Nguyen, JP, Brugières, P, Lefaucheur, JP, Bourdet, C *et al.* (2000). Motor and cognitive improvements in patients with Huntington's disease after neural transplantation. *Lancet* **356**: 1975–1979.
89. Gaura, V, Bachoud-Lévi, AC, Ribeiro, MJ, Nguyen, JP, Frouin, V, Baudic, S *et al.* (2004). Striatal neural grafting improves cortical metabolism in Huntington's disease patients. *Brain* **127**(Pt 1): 65–72.
90. Dunnett, SB and Rosser, AE (2011). Clinical translation of cell transplantation in the brain. *Curr Opin Organ Transplant* **16**: 632–639.
91. Dunnett, SB and Rosser, AE (2011). Cell-based treatments for huntington's disease. *Int Rev Neurobiol* **98**: 483–508.
92. Zietlow, R, Lane, EL, Dunnett, SB and Rosser, AE (2008). Human stem cells for CNS repair. *Cell Tissue Res* **331**: 301–322.
93. Dunnett, SB and Rosser, AE (2007). Stem cell transplantation for Huntington's disease. *Exp Neurol* **203**: 279–292.
94. Ogawa, R, Mizuno, H, Watanabe, A, Migita, M, Hyakusoku, H and Shimada, T (2004). Adipogenic differentiation by adipose-derived stem cells harvested from GFP transgenic mice-including relationship of sex differences. *Biochem Biophys Res Commun* **319**: 511–517.
95. Olson, SD, Kambal, A, Pollock, K, Mitchell, GM, Stewart, H, Kalomoiris, S *et al.* (2012). Examination of mesenchymal stem cell-mediated RNAi transfer to Huntington's disease affected neuronal cells for reduction of huntingtin. *Mol Cell Neurosci* **49**: 271–281.
96. Beegle, J, Lakatos, K, Kalomoiris, S, Stewart, H, Isseroff, RR, Nolta, JA *et al.* (2015). Hypoxic preconditioning of mesenchymal stromal cells induces metabolic changes, enhances survival, and promotes cell retention in vivo. *Stem Cells* **33**: 1818–1828.
97. Rosová, I, Dao, M, Capoccia, B, Link, D and Nolta, JA (2008). Hypoxic preconditioning results in increased motility and improved therapeutic potential of human mesenchymal stem cells. *Stem Cells* **26**: 2173–2182.